J Therm Spray Tech (2018) 27:1388–1400
https://doi.org/10.1007/s11666-018-0746-7

CrossMark

PEER REVIEWED

Enhancing Biocompatibility and Corrosion Resistance of Ti-6Al-4V Alloy by Surface Modification Route

Tejinder Pal Singh Sarao[1] · Harpreet Singh[2] · Hazoor Singh[3]

Submitted: 18 June 2018 / in revised form: 27 July 2018 / Published online: 17 August 2018
© ASM International 2018

Abstract Titanium (Ti) and its alloys are widely used as candidate materials for biomedical implants. Despite their good biocompatibility and corrosion resistance, these materials suffer from corrosion after implantation in biological environments. The aim of this research work is to study the effect of two coatings on biocompatibility and corrosion behavior of Ti-6Al-4V biomedical implant material. Hydroxyapatite (HA) and hydroxyapatite/titanium dioxide (HA/TiO_2) coatings were thermal-sprayed on Ti-6Al-4V substrates. In the latter case, TiO_2 was used as a bond coat between the substrate and HA top coat. The corrosion behavior of coated and un-coated samples in Ringer's solution was studied by potentiodynamic and linear polarization techniques. Before and after corrosion testing, XRD and SEM/EDS techniques were used for the analysis of phases formed and to investigate microstructure/compositional changes in the coated specimens. The cellular response was analyzed by the MTT (microculture tetrazolium) assay. The results showed that both the HA, as well as, the HA/TiO_2 coatings significantly increased the corrosion resistance of the substrate material. The HA coating was found to be more biocompatible as compared to the un-coated and HA/TiO_2-coated Ti-6Al-4V alloy.

✉ Harpreet Singh
harpreetsingh@iitrpr.ac.in

[1] Baba Farid College of Engineering and Technology, Bathinda, Punjab, India

[2] Indian Institute of Technology Ropar, Rupnagar, Punjab, India

[3] Yadavindra College of Engineering, Talwandisabo, Punjab, India

Keywords corrosion · cell culture · HA · in vitro · TiO_2 · thermal spray coating

Introduction

The worldwide increase in the average age of people has led to the increase in demand of biomedical implants (Ref 1). Approximately, one million orthopedic implant surgeries in association with total joint replacements are needed yearly. This number is expected to double between 1999 and 2025 due to continuous increase in musculoskeletal injuries and diseases (Ref 1). Metals and alloys are used as biomedical implants in clinical applications due to their excellent mechanical properties. The purpose of metallic implants is to support the newly formed bone during physiologic loading (Ref 2). Ti-based alloys are preferred in biomedical applications as their modulus of elasticity is lower and closer to that of human bone in comparison with stainless steel and Co-Cr alloys (Ref 3). However, degradation occurs when these materials are used in the highly corrosive human body environment. The human body, with an oxygenated saline solution of 0.9% salt content at pH 7.4 and temperature 37 °C, is a harsh environment for metals and alloys. Most metallic materials undergo chemical or electrochemical dissolution due to the harsh and corrosive environment of the human body (Ref 4). The presence of amino acids and proteins in the body fluids accelerates corrosion. Extensive release of ions can result in adverse biological reactions in the body and can lead to mechanical failure of the implant (Ref 5).

There are several studies that address the corrosion of metallic implants. Hallab et al. (Ref 6) reported that almost all the metals in contact with biological systems undergo corrosion. In a study (Ref 7) of 148 retrieved Ti6Al4V/Co-

Cr and Co-Cr/Co-Cr modular hip prostheses, significant corrosion was observed in the conical taper region between the head and stem. Mathiesen et al. (Ref 8) suggested that the crevice between the head and neck is a potential site of corrosion in modular hip prostheses. Grupp et al. (Ref 9) studied the modular Ti6A14V alloy, neck adapter failures in hip replacements. It was found that surface cracks formed due to fretting corrosion led to fatigue fracture of the Ti6A14V modular neck adapters. Goldberg et al. (Ref 10) in a multicenter retrieval analysis of 231 modular hip implants observed moderate-to-severe corrosion in 28% of the heads of similar alloy couples and 42% of the heads of mixed alloy couples. It was found that *in vivo* corrosion of modular hip taper interfaces is due to a mechanically assisted crevice corrosion process. The fretting corrosion of the contact areas between screws and plates made of dissimilar metals in both human serum and Hank's solution was investigated by Hol et al. (Ref 11). It was found that titanium screws and plates corroded more in serum than in saline, while the opposite was true for stainless steel.

Ti-6Al-4V alloy is preferred as an implant biomaterial due to its high mechanical strength (Ref 12). Surface modification of metallic implants with a bioactive coating can be an attractive solution for the degradation problems (Ref 13). Moreover, this will also help in the bone growth for successful implantation. Calcium phosphate-based HA is widely used as a surface coating on metallic implants due to its excellent biocompatibility (Ref 2). Plasma spraying is the most preferred technique for deposition of HA coatings on implant biomaterials (Ref 14, 15). In plasma-sprayed coatings, HA particles melt completely or partially owing to high temperature of the plasma (Ref 15). It leads to the formation of some undesirable phases, which dissolve faster than HA in body fluids and lead to mechanical degradation of the coating (Ref 15). To overcome the problems of existing plasma-sprayed HA coatings, a number of surface modification techniques have been proposed by several researchers (Ref 16-18). However, optimum coating properties are still to be achieved to create more stable HA coatings.

Titania, TiO_2, is preferred as a composite or bond coat with HA due to its corrosion resistance and biological properties (Ref 19-21). The aim of the present study was to develop HA and HA/TiO_2 coatings on extra low interstitial Ti-6Al-4V alloy. Titania has been chosen as a bond coat material with HA coatings. Subsequently, the aim was to investigate the corrosion behavior of the substrate material after deposition of the coatings in Ringer's solution. The biological response of the coatings was investigated by the in vitro cell culture experiments. A High-Velocity Flame Spray (HVFS) technique has been used for the current investigation to develop HA and HA/TiO_2 coatings on Ti-6Al-4V substrates. This is an innovative thermal spray technique which is characterized by high particle velocity and low flame temperature in comparison with the plasma spraying. This is a simple and cost-effective technique in comparison with other thermal spray techniques.

Experimentation

Material and Methods

Commercially available biomedical material ASTM F136 grade titanium-aluminum-vanadium alloy, Ti-6Al-4V, has been used as the substrate material in this study. Ti-6Al-4V is one of the most commonly used Ti alloys, which is an alpha-beta alloy containing 6% Al and 4% V. In Ti-6Al-4V, the interstitial elements of iron and oxygen are carefully controlled to improve ductility and fracture toughness. The chemical composition of the substrate material is given in Table 1. Ti-6Al-4V disk-shaped specimens each measuring 12 mm × 5 mm were prepared. The specimens were polished by different grades of silicon carbide papers (180-1200 grit) followed by cloth wheel polishing with alumina paste on a polishing machine. These specimens were washed with de-ionized water followed by acetone rinsing. The HA (Captal 30, Plasma Biotal Ltd. UK) and TiO_2 (Amperit 782.0, H.C. Starck GmbH & Co. KG, Goslar, Germany) powders were used in this study. The substrates were grit blasted with alumina (Al_2O_3) in accordance with normal thermal spray practice to achieve a strong bond between the coating and substrate. The substrates were subsequently air-blasted to remove any residual grit. The air-blasted specimens were then coated with the HA and HA/TiO_2 powders using HVFS technique. It is specially designed thermal spraying equipment (CERAJET). This is a modified version of the conventional powder flame spray system. CERAJET is a proprietary product of Metalizing Equipment Company Private Limited (MECPL) Jodhpur, India. The details about coating deposition technique and process parameters are already published elsewhere (Ref 21).

Characterization of the Coatings

The phase composition of the as-sprayed coatings was studied by X'pert-PRO XRD instrument utilizing Cu K_α x-ray source, operating at 40 kV/30 mA. A surface as well

Table 1 Chemical composition of Ti-6Al-4V alloy

Element	N	C	H	O	Fe	Al	V	Ti
wt.%	0.02	0.05	0.01	0.16	0.20	6.10	3.95	Balance

as a cross-sectional SEM/EDS analysis of the coated samples was performed using a FEI Quanta 200F, SEM instrument connected with an EDS system. EDS point analysis provides the composition (in at.%) of elements in the coating. Samples were sectioned with a low-speed precision saw and mounted in epoxy resin for cross-sectional SEM/EDS analysis of the coatings. Mounted samples were polished with emery papers of different grades. Subsequently, the specimens were mirror polished with slurry of alumina on a napped cloth. EDS mapping was carried out to display the distribution of main elements in the coating as well as substrate. The surface roughness of materials is an important parameter in biomedical application. The surface roughness (R_a) and standard deviation values of Al_2O_3 blasted, HA-coated, and HA/TiO_2 bond-coated Ti-6Al-4V samples were measured by a Surftest SJ-400 surface roughness tester (Mitutoyo Corporation, Japan) as per roughness standard JIS1994.

In Vitro Corrosion and Cell Culture Studies

To investigate the corrosion behavior of the un-coated, HA-coated, and HA/TiO_2-bond-coated Ti-6Al-4V specimens in Ringer's solution, a potentiodynamic polarization test was conducted using a G-750; Gamry Instruments Potentiostat/Galvanostat. The chemical composition of Ringer's solution was (in g/L) 0.9-NaCl, 0.24-$CaCl_2$, 0.43-KCl, and 0.2-$NaHCO_3$ at pH 7.2. The corrosion rate was determined using the Tafel extrapolation method. Linear polarization technique was used to measure the polarization resistance (R_p) of the coated and un-coated samples. All the tests were performed on fresh samples by exposing 1 cm^2 area of sample in Ringer's solution. The average value of three measurements was reported in the results. After corrosion testing, the specimens were further analyzed by XRD and SEM/EDS techniques for identification of different phases formed and microstructure/compositional analysis.

In vitro cell culture studies were carried out to evaluate the biological behavior of the flame-sprayed coatings. Human osteosarcoma cell line KHOS-NP (R-970-5) supplied by NCCS (National Centre for Cell Science, India) has been used for this purpose. These cells were seeded on polystyrene culture plates (control), HA, and HA/TiO_2-bond-coated and un-coated Ti-6Al-4V (blasted) samples. All the samples were placed in twelve well plates separately at a density of 1×10^3 cells/well with 3 mL of the culture medium in each well. In control, the cells were placed directly into twelve well plates. The culture medium consisted of Dulbecco's modified Eagle's medium (DMEM) supplemented with 10% fetal bovine serum (FBS) and 1 mM nonessential amino acid solution. These cell seeded samples were incubated for 14 days at 37 °C in a humidified incubator with 5% CO_2. Media was changed after every two days. After 7 and 14 days of incubation, the cell proliferation was studied by methyl thiazolyl blue tetrazolium (MTT) assay. For MTT assay, the 500 µL culture from each cell plate was transferred to fresh plates, and 100 µL of MTT was added to each plate. 800 µL lysis buffer (20% sodium dodecyl sulfate, 50% dimethyl formamide, and 30% distilled water) was added to each well, mixed, and incubated at 37 °C for 2 h. The absorbance of the solution at 570 nm (A_{570}) was measured using UV–Vis spectrophotometer (Make: Germany). All MTT assays were performed in triplicate.

Results and Discussion

XRD Analysis

The XRD patterns for the as-sprayed HA and HA/TiO_2 coatings on Ti-6Al-4V substrates are shown in Fig. 1. The XRD patterns were obtained for 20°-60° range of 2θ values as it covers the major peaks of Ti and HA. The most intense peak for HA and HA/TiO_2 coatings on Ti-6Al-4V substrate was observed at 31.9° (2θ), which indicates the strongest peak for HA as per JCPDS card no. 9-432. The peaks for tetracalcium phosphate $Ca_4(PO_4)_2O$ (TTCP) and β-tricalcium phosphate $Ca_3(PO_4)_2$ (β-TCP) phases are compared with standard JCPDS data cards 25-1137 and 9-169, respectively. The melting temperature of HA is

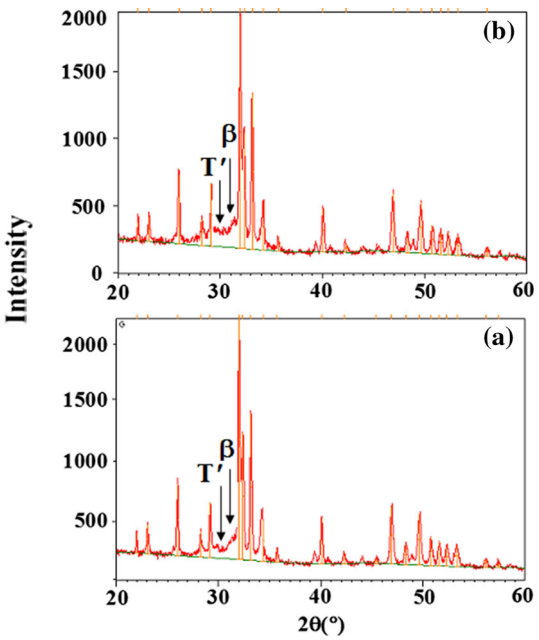

Fig. 1 XRD pattern of as-sprayed (a) HA and (b) HA/TiO_2 coatings on Ti-6Al-4V alloy [TTCP (T'), β-TCP (β), and HA (unmarked peaks)]

1550 °C, however above 1050 °C HA decomposes into β-TCP and TTCP phases (Ref 22). The following reactions may occur in the decomposition (Ref 22-24).

$$Ca_{10}(PO_4)_6(OH)_2 \rightarrow Ca_{10}(PO_4)_6(OH)_{2-2x}O_xV_x + xH_2O \quad \text{(Eq 1)}$$

$$Ca_{10}(PO_4)_6(OH)_{2-2x}O_xV_x \rightarrow Ca_{10}(PO_4)_6O_xV_x + (1-x)H_2O \quad \text{(Eq 2)}$$

$$Ca_{10}(PO_4)_6O_xV_x \rightarrow 2Ca_3(PO_4)_2 + Ca_4(PO_4)_2O \quad \text{(Eq 3)}$$

The decomposition of HA coatings is related to the high temperature in thermal spraying flame. It has been reported that in thermal-sprayed HA coatings, process-related variability shows significant effect on coating characteristics such as phase composition, structure and chemical composition (Ref 25). Both HA and HA/TiO_2 coatings on the Ti-6Al-4V substrates are observed to be highly crystalline, which may be due to the presence of higher percentage of un-melted HA powder particles during flame spraying. No XRD peak of TiO_2 was detected on the HA/TiO_2-coated Ti-6Al-4V substrate surface. It shows that intermediate bond coat of TiO_2 is completely covered by HA top coat.

SEM/EDS Analysis

SEM micrographs of as-sprayed HA and HA/TiO_2 coatings along with EDS point analysis on Ti-6Al-4V substrates are shown in Fig. 2 and 3, respectively. The microstructure of HA coating consists of fully molten splats while HA/TiO_2 coating showed a typical splat-like morphology. The splats are observed to have deformed significantly during impact. The EDS point analysis of HA and HA/TiO_2 coatings on Ti-6Al-4V substrates confirm the presence of calcium (Ca), phosphorous (P), and oxygen (O) elements in the coating.

In previous studies (Ref 26-28), other researchers reported the presence of Ca, P, O and C elements in the CaP-based coatings. The initial HA powder has a Ca/P atomic ratio of 1.67. The observed Ca/P ratios for both the coatings confirm the presence of additional phases other than HA. There are no indications of titanium on the surface of HA/TiO_2-coated Ti-6Al-4V substrate. It shows that the bond coat of TiO_2 is completely covered with a HA top coat. The calculated Ca/P ratios from EDS spectra for the as-sprayed HA and HA/TiO_2 coatings are tabulated in Table 2. The Ca/P ratio of 1.68 (at point 1 in Fig. 3) and 1.64 (at point 2 in Fig. 2) is in good agreement with the stoichiometric HA (Ca/P ratio = 1.67). The Ca/P ratio of 1.52 (at point 3 in Fig. 2 and 3) indicates the formation of TCP phase. The presence of both HA and TCP phases is also confirmed by the XRD analysis. Romain et al. (Ref 29) also reported the Ca/P ratio between 1.5 and 2.2 for the suspension plasma-sprayed HA coatings, which indicated the presence of TCP, TTCP, HA and CaO compounds. Snyders et al. (Ref 30) with Ca/P ratio of 1.51 ± 0.02-1.82 ± 0.02 also reported the formation of TCP, HA and CaO phases in the radio frequency (RF) sputtered HA coatings. In a suspension plasma-sprayed HA coating study (Ref 31), different Ca/P ratios showed the presence of HA, β-TCP, TTCP and CaO phases.

The cross-sectional micrograph along with the corresponding EDS maps of as-sprayed HA and HA/TiO_2 coatings on Ti-6Al-4V substrate are shown in Fig. 4 and 5, respectively. The average value of the coating thickness measured from the cross-sectional micrograph of HA coating is 135 µm. From the EDS maps of HA coatings,

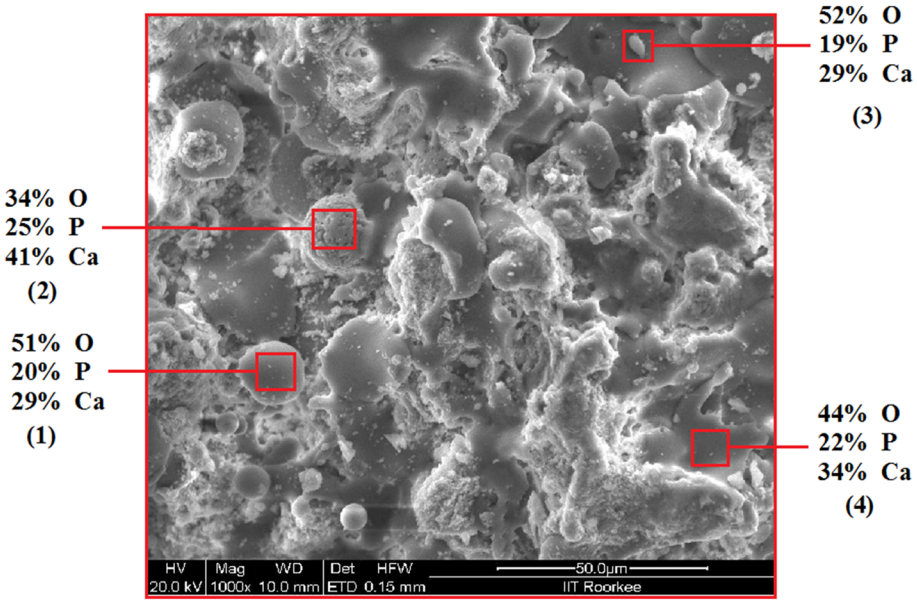

Fig. 2 FE-SEM analysis along with EDS point analysis showing elemental composition of as-sprayed HA coating on Ti-6Al-4V alloy

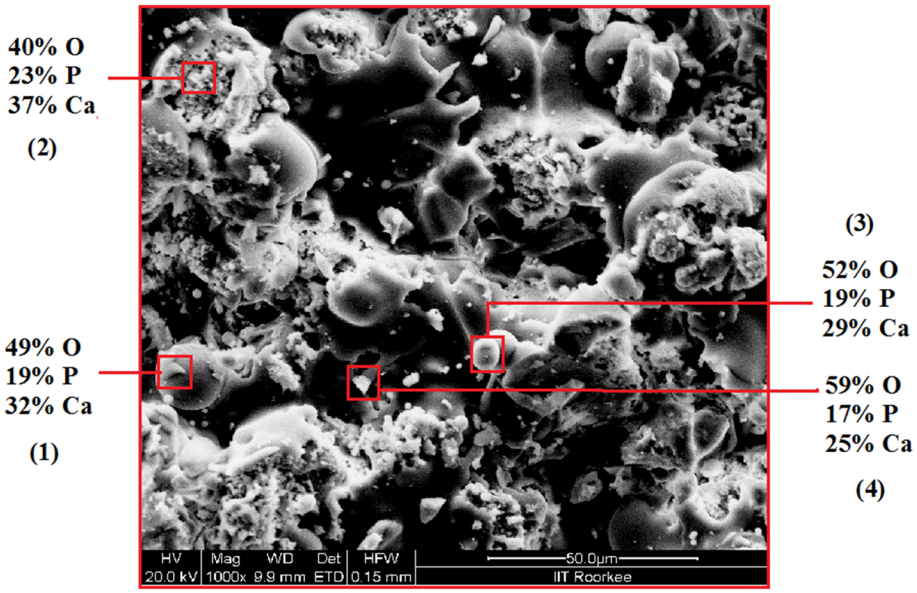

Fig. 3 FE-SEM analysis along with EDS point analysis showing the elemental composition of as-sprayed HA/TiO_2 coating on Ti-6Al-4V alloy

Table 2 Ca/P ratios of as-sprayed hydroxyapatite (HA) and hydroxyapatite/titanium dioxide (HA/TiO_2) coatings on Ti-6Al-4V alloy

Coating	Point 1	Point 2	Point 3
HA coating (Fig. 2)	1.45	1.64	1.52
HA/TiO_2 coating (Fig. 3)	1.68	1.60	1.52

the distribution of Ca and P elements seems to be homogenous with the presence of O throughout the coating. The coating has a typical splat-like laminar morphology, and is dense and adherent to the Ti-6Al-4V substrate. The coating thicknesses measured from the cross-sectional micrograph of the HA/TiO_2 coating (Fig. 5), are 120 and 20 µm, respectively, for the HA top coat and TiO_2 bond coat. The mappings of Ca and P elements in the top coat and Ti elements in the bond coat clearly demonstrated that the elements are uniformly distributed in the coating. TiO_2 intermediate layer appears intact and well adhered to Ti-6Al-4V substrate.

Surface Roughness

Roughness of implant surface is one of the most important characteristic which further influences the osseointegration. The surface roughness was measured at five different positions for each sample and the average value was used as the indicator of the roughness. The average surface roughness (R_a) value for the un-coated Ti-6Al-4V (blasted) substrates was 4.0 ± 0.4 µm. The HA and HA/TiO_2 coatings have the surface roughness values of 4.6 ± 0.2 and 5.9 ± 0.4 µm. The roughness of Ti-6Al-4V substrate increased after coating deposition. The increase in roughness of HA/TiO_2 coating in comparison with HA coating may be attributed to the presence of the TiO_2 intermediate layer in the HA/TiO_2 coating. High surface roughness of HA coatings leads to the increase in dissolution rate and facilitates apatite precipitation (Ref 32).

It is pertinent to mention that the particle size of feedstock powder also affects the coating surface roughness (Ref 33-35). The surface roughness of as-sprayed coatings supports the roughness values given by Gross and Muller (Ref 33), who reported that thermal-sprayed HA coatings with a powder particle size of 20-40, 40-60 and 60-80 µm, respectively, gives R_a values of 4.8, 7.4 and 9.5 µm, respectively. The average particle size of HA powder used in the present study is 30 µm.

In vitro Corrosion Studies

The potentiodynamic polarization curves of coated and un-coated Ti-6Al-4V specimens in Ringer's solution at 37 ± 1 °C temperature are depicted in Fig. 6. The pH of the Ringer's solution was maintained around 7.2 as the changes in pH influence the corrosion behavior (Ref 3). The corrosion parameters determined from the potentiodynamic curves for coated and un-coated Ti-6Al-4V specimens by Tafel extrapolation method are summarized in Table 3. The corrosion parameters are anodic Tafel slope (β_a), cathodic Tafel slope (β_c), corrosion potential (E_{corr}), corrosion current density (I_{Corr}) and corrosion rate (C_R). Polarization resistance (R_p) values determined from linear polarization tests for coated and un-coated Ti-6Al-4V specimens are also compiled in Table 3. The analysis of Tafel slope values shows that among the investigated cases,

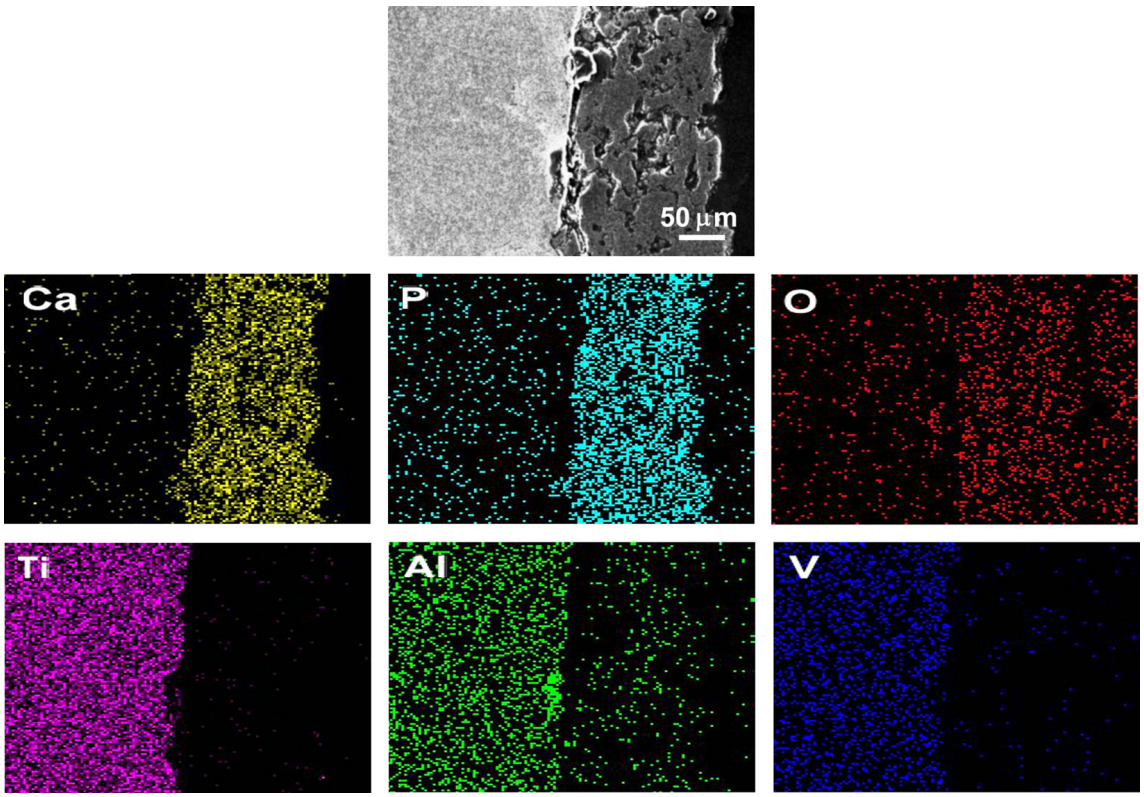

Fig. 4 Cross-sectional SEM and EDS elemental maps of as-sprayed HA coating on Ti-6Al-4V alloy (scale bar = 50 μm)

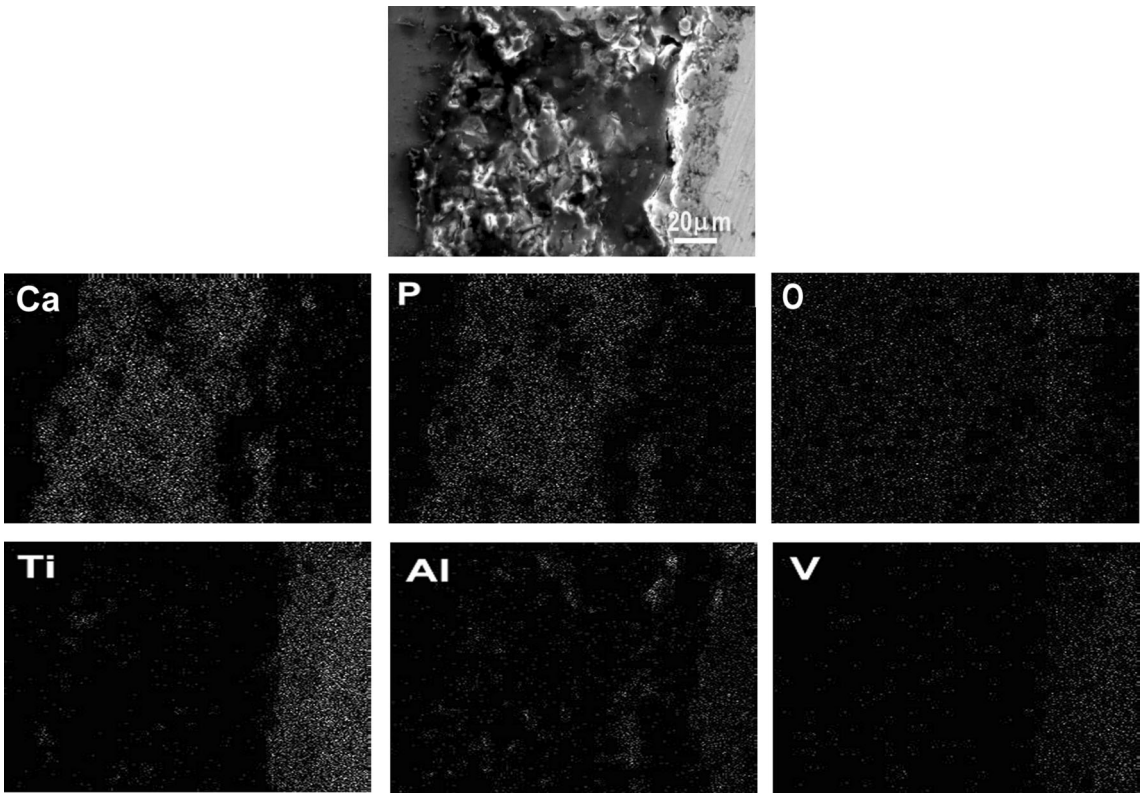

Fig. 5 Cross-sectional SEM and EDS elemental maps of as-sprayed HA/TiO_2 coating on Ti-6Al-4V alloy (scale bar = 20 μm)

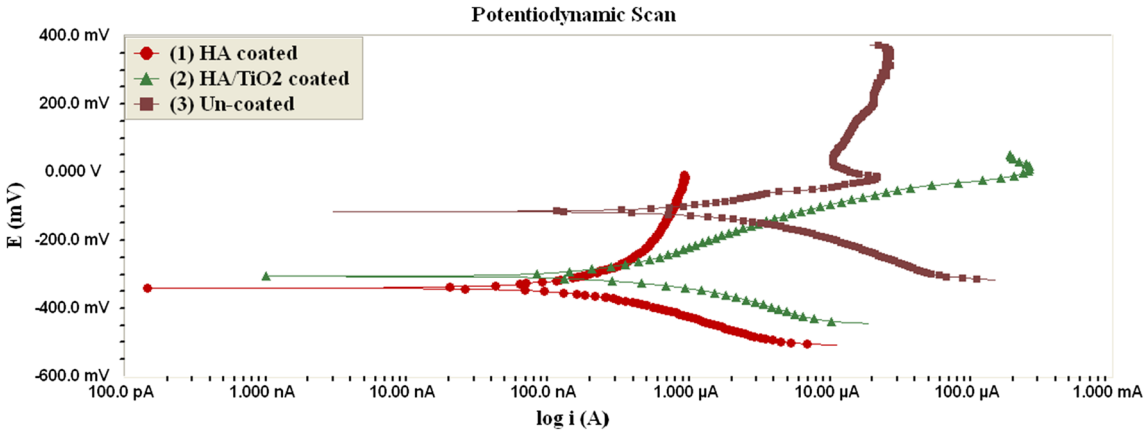

Fig. 6 Potentiodynamic curves of flame-sprayed (1) HA-coated (2) HA/TiO_2-coated (3) un-coated, Ti-6Al-4V alloy specimens in Ringer's solution at 37 ± 1 °C temperature

corrosion current density of un-coated Ti-6Al-4V (I_{Corr} = 1.200 µA cm^{-2}, E_{Corr} = − 116 mV) is higher than HA-coated (I_{Corr} = 0.167 µA cm^{-2}, E_{Corr} = − 340 mV) and HA/TiO_2-coated (I_{Corr} = 0.394 µA cm^{-2}, E_{Corr} = − 305 mV) Ti-6Al-4V specimens in Ringer's solution. The potentiodynamic polarization curve for un-coated Ti-6Al-4V specimen was found to get shifted toward the right in comparison with the potentiodynamic curves for HA and HA/TiO_2-coated specimens. All I_{Corr} values reflect good corrosion resistance, including un-coated Ti-6Al-4V specimen; however, it can be deduced through this study that HA and HA/TiO_2 coatings have improved the corrosion resistance of the un-coated specimens. HA-coated Ti-6Al-4V specimen showed a lowest corrosion rate (0.0014 mm/year), while the un-coated Ti-6Al-4V specimen exhibited a highest corrosion rate (0.0102 mm/year) in Ringer's solution.

The polarization resistance values (Table 3) for the Ti-6Al-4V specimens also showed the similar trends for corrosion behavior of the specimens. Un-coated Ti-6Al-4V specimens showed a lowest polarization resistance (R_p = 6.23 KΩ cm^2), while HA-coated Ti-6Al-4V specimens showed a highest polarization resistance (R_p = 24.80 KΩ cm^2). The higher the value of R_p, more resistant is the material to corrode. Based upon these values, it can again be concluded that un-coated Ti-6Al-4V has suffered from highest corrosion, while HA-coated Ti-6Al-4V specimens have shown a lowest corrosion rate. All the above results clearly indicate the protective behavior of deposited coatings. Surface modification effectively enhanced the corrosion resistance of Ti6Al4V specimens.

These results agree with other investigations in which HA-, TiO_2- and ZrO_2-coated specimens showed improvement in corrosion resistance in comparison with un-coated specimens (Ref 36-38). On the contrary, Kumari et al. (Ref 39) reported the increase in corrosion rate of plasma-sprayed (HA-TiO_2) composite coated Ti-6Al-4V specimens. The decrease in corrosion resistance of coated specimens in comparison with as-received specimens was attributed to the presence of partially amorphous phases in as-sprayed HA-TiO_2 coating. It is a well known fact that amorphous HA coating dissolves rapidly in simulated body fluids. Kwok et al. (Ref 40) also reported an improvement in corrosion resistance of the HA-coated Ti-6Al-4V in comparison with as-received Ti-6Al-4V alloy substrate. Fathi and Azam (Ref 41) found that HA/Tantalum coated specimen was more corrosion resistant than the un-coated 316L SS specimen in the normal saline solution and Ringer's solution. Valereto et al. (Ref 42) studied the corrosion behavior of un-coated and plasma spray HA-coated Ti-6Al-7Nb substrates in Hank's solution. They found that corrosion rate of un-coated substrates was two times lower than HA-coated substrates. The higher corrosion of coated substrates was suggested to be associated with porosity in HA coatings.

The XRD diffractograms of flame-sprayed HA and HA/TiO_2 coatings on Ti-6Al-4V after immersion in Ringer's solution are depicted in Fig. 7. XRD was conducted on the coatings to identify the phase changes after corrosion testing. The XRD analysis confirmed the presence of HA, with minor peaks for TTCP and β-TCP phases on both coatings. All the main peaks correspond to HA as a dominant phase. Diffractograms showed no apparent change in the phase composition of the coatings after their immersion. Coatings appeared more crystalline, and it was found that after immersion, the intensity of XRD peaks increased in comparison with as-sprayed HA and HA/TiO_2 coatings (Fig. 1). Earlier, Kim et al. (Ref 43) and Lu et al. (Ref 44) reported that a dense and highly crystalline coating effectively shields the release of metallic ions from the implant into the body.

Table 3 Corrosion parameters of coated and un-coated Ti-6Al-4V alloy in Ringer's solution at 37 ± 1 °C temperature

Parameters	HA	HA/TiO_2	Un-coated
β_a, e^{-3} V/decade	221.1	364.7	112.2
β_c, e^{-3} V/decade	77.10	430.4	64.50
E_{Corr}, mV	− 340	− 305	− 116
I_{Corr}, μA cm^{-2}	0.167	0.394	1.200
C_R, mm/year	0.0014	0.0033	0.0102
R_p, KΩ cm^2	24.80	11.70	06.23

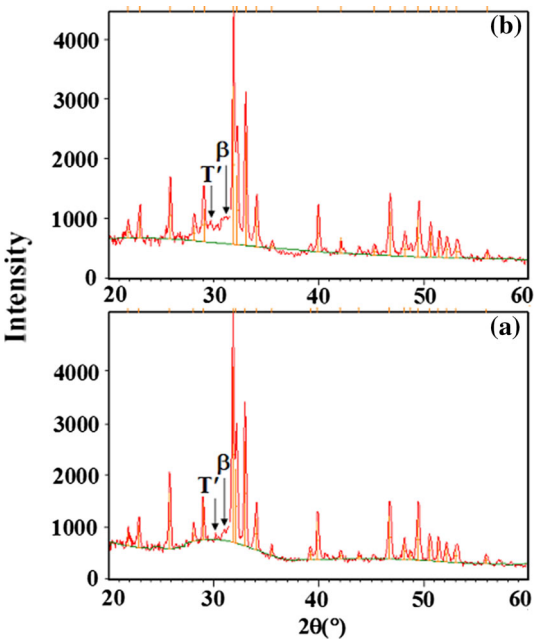

Fig. 7 XRD pattern of flame-sprayed (a) HA and (b) HA/TiO_2 coatings on Ti-6Al-4V alloy after immersion in Ringer's solution [TTCP (T′), β-TCP (β), and HA (unmarked peaks)]

The microstructure of HA- and HA/TiO_2-coated Ti-6Al-4V (Fig. 8 and 9), after immersion in Ringer's solution consists of well-flattened splats with the presence of some spherical-shaped particles. In EDS point analysis, C and O have been detected as the predominant elements after corrosion testing in both coatings. No visible cracks were observed on HA-coated Ti-6Al-4V (Fig. 8); however, few microcracks can be observed on the surface of HA/TiO_2-coated Ti-6Al-4V specimen (Fig. 9). However, point analysis confirmed that Ti was not present on the surface of HA/TiO_2 coatings. It shows that bond coat of TiO_2 remained intact with the HA top coat even after exposure of coating to Ringer's solution. The microcracks may act as active sites for the incursion of pitting corrosion. However, no such pit was observed on the surface of any specimen after electrochemical corrosion testing. It seems that HA/TiO_2-coated Ti-6Al-4V substrate surface was entirely protected by the intermediate TiO_2 layer between the base substrate and HA top coating. TiO_2 layer behaved as an additional barrier to the flow of ions between the Ringer's solution and Ti-6Al-4V substrate.

The calculated Ca/P ratio from EDS spectra for the HA- and HA/TiO_2-coated specimens at different points after corrosion testing are tabulated in Table 4. The results indicate reduction in Ca/P ratios in both coatings after immersion compared to as-sprayed coatings (Table 2). The decrease in Ca/P ratio indicates the dissolution of HA in Ringer's solution. A Ca/P ratio of 1.37 in HA coating (at point 1 in Fig. 8) is very close to Ca/P ratio of 1.33, which supports the formation of octocalcium phosphate (OCP). Ca/P ratio of 1.00 (at point 2 in Fig. 8 and at point 3 in Fig. 9) indicates the formation of dicalcium phosphate anhydrous (DCPA) and dicalcium phosphate dihydrate (DCPD). These are not desirable phases due to their higher dissolution rate after implantation. A comparison of EDS analysis of both HA- and HA/TiO_2-coated Ti-6Al-4V

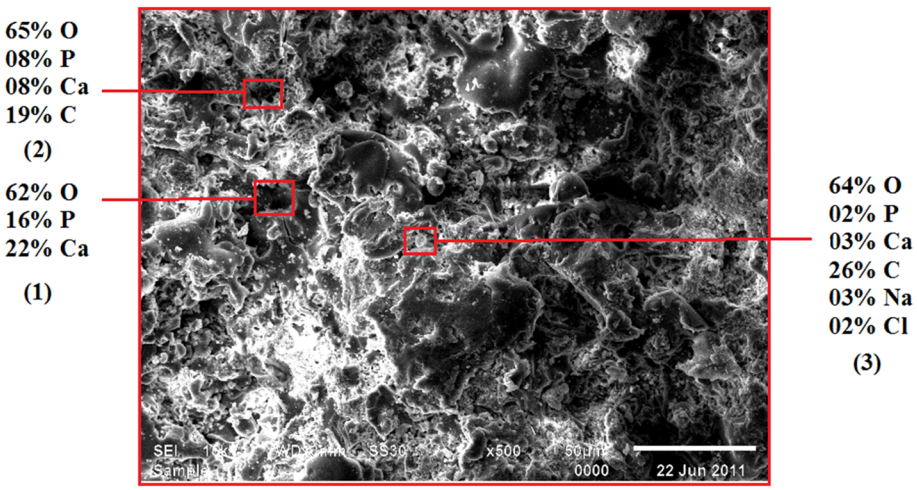

Fig. 8 FE-SEM along with EDS point analysis of flame-sprayed HA-coated Ti-6Al-4V alloy after immersion in Ringer's solution

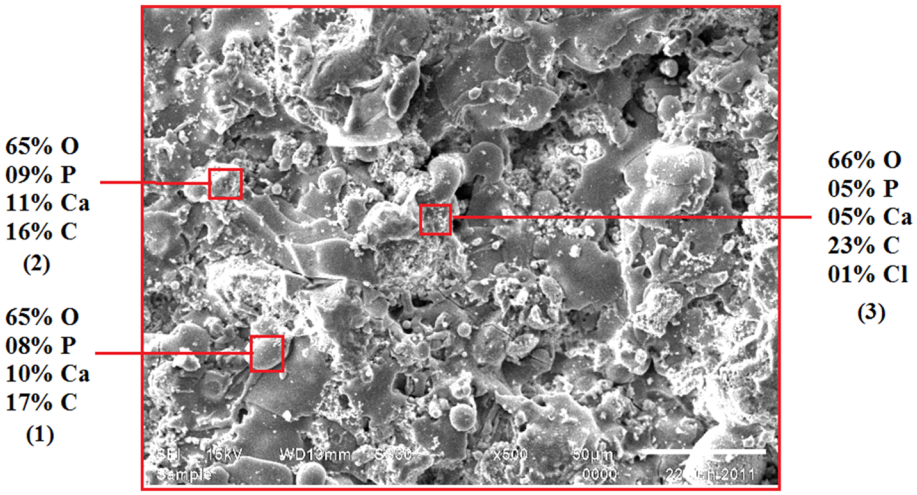

Fig. 9 FE-SEM along with EDS point analysis of flame-sprayed HA/TiO_2-coated Ti-6Al-4V alloy after immersion in Ringer's solution

Table 4 Ca/P ratios of hydroxyapatite (HA) and hydroxyapatite/titanium dioxide (HA/TiO_2) coatings on Ti-6Al-4V alloy after immersion in Ringer's solution

Coating	Point 1	Point 2	Point 3
HA coating (Fig. 8)	1.37	1.00	1.5
HA/TiO_2 coating (Fig. 9)	1.25	1.22	1.00

specimens before and after corrosion testing shows that the atomic percentage of Ca and P has decreased, whereas that of O increased after their immersion in Ringer's solution. The dominance of O in the composition indicates the onset of oxidation. No evidence of pitting corrosion was detected on the exposed un-coated Ti-6Al-4V alloy. The corrosion resistance of un-coated Ti-6Al-4V alloy may be attributed to the protective oxide layer on the substrate surface after immersion. The cross-sectional SEM and EDS maps of the HA and HA/TiO_2 coatings on the Ti-6Al-4V specimen after corrosion testing in Ringer's solution are shown in Fig. 10 and 11, respectively. The cross-sectional analysis of HA coatings on Ti-6Al-4V (Fig. 10) indicates a dense coating with the presence Ca and P elements. The coating, by and large, has retained its identity. Ti, Al and V are restricted to the base substrate. The coating–substrate interface seems to be defect-free and intact in the HA coating on Ti-6Al-4V. The EDS maps of as-sprayed (Fig. 4) and exposed (Fig. 10) specimens of HA-coated Ti-6Al-4V have not shown any significant differences. In the EDS maps of HA/TiO_2 coating on Ti6Al4V specimen (Fig. 11), TiO_2 bond layer has retained its adhesion to the base substrate and top HA coating even after immersion in Ringer's solution. Ti elemental map represent both the bond coat as well as the substrate.

In Vitro Cell Culture Studies

In the present work, in vitro cell culture tests were conducted to investigate the biological response of different specimens using human osteosarcoma cell line. Osteosarcoma is a primary malignant bone tumor which mostly affects the children and adolescents (Ref 45). Cell culture is a complex process, in which cells are grown in vitro under controlled conditions. The purpose of in vitro cell culture testing of implant materials under controlled conditions is to analyze their cell response prior to their use in the in vivo environment. Cells were seeded on polystyrene culture plates, HA, HA/TiO_2-coated and un-coated Ti-6Al-4V (blasted) samples. Polystyrene culture plate was used as control. Cell proliferation is a fundamental measurement of cell response which has been monitored by the MTT assay in the current study. The results of MTT assays after 7 and 14 days are shown in Fig. 12. MTT assay results revealed that the cells proliferated on all of the tested samples over a period of 7 and 14 days. After 7 days of incubation, cells on culture plates, HA- and HA/TiO_2-coated Ti-6Al-4V specimens proliferated favorably. Polystyrene cell culture plates showed the highest rate of proliferation compared to the other specimens after 14 days, whereas HA coatings have shown almost similar results. It can be concluded from the in vitro cell culture analysis that both coatings are significantly more bioactive than bare Ti-6Al-4V specimens and can play an effective role to enhance the performance of the given implants.

It has been observed from MTT studies that HA- and HA/TiO_2-coated specimens exhibited a higher proliferation in comparison with un-coated Ti-6Al-4V specimens, after 7 and 14 days of incubation. These differences were also evident after 14 days of incubation. Rate of cell proliferation was faster within first 7 days of incubation on all the samples as shown by the absorbance values. HA-coated samples

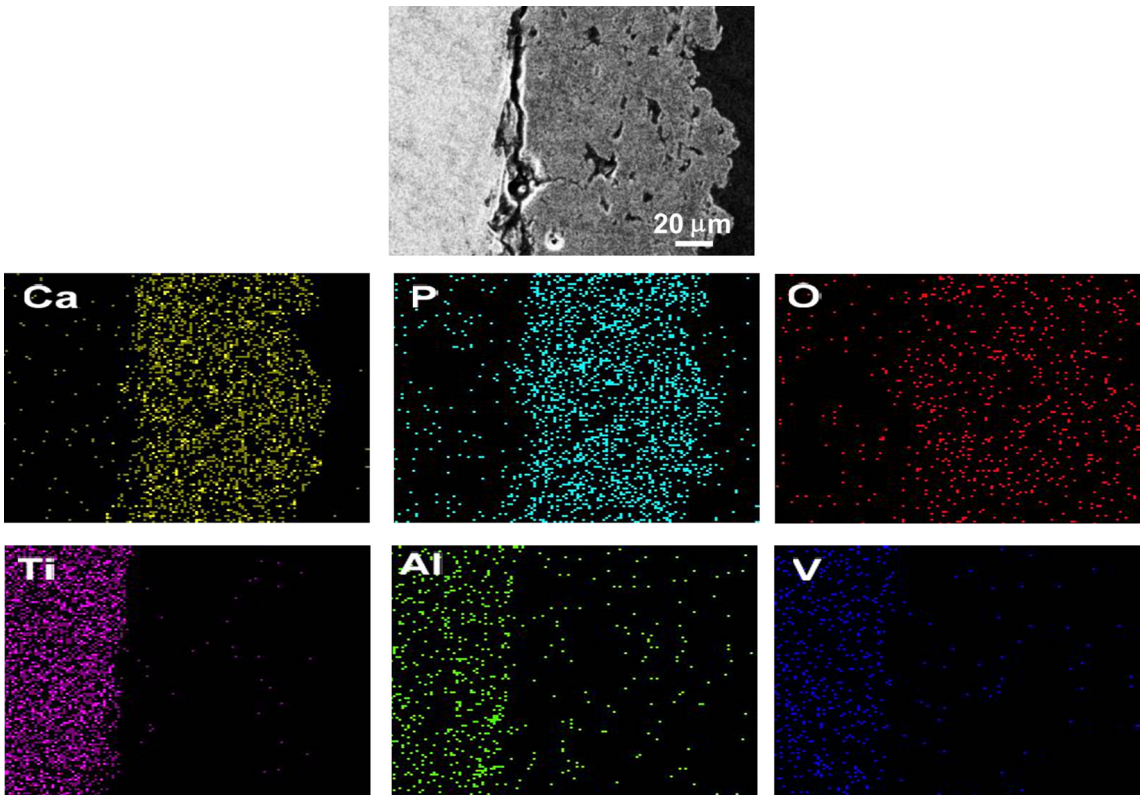

Fig. 10 Cross-sectional EDS elemental maps of flame-sprayed HA-coated Ti-6Al-4V alloy after immersion in Ringer's solution (scale bar = 20 µm)

indicated a higher number of living cells after 14 days, that is, increased cell proliferation results, while the number of the living cells was significantly lower on un-coated Ti-6Al-4V samples. As the cell proliferation difference is marginal between HA- and HA/TiO_2-coated specimens, it may be due to the presence of HA as top coat in both coatings. Rad et al. (Ref 46) also revealed increase in the cell proliferation of HA-coated Ti substrates in comparison with un-coated Ti substrates. Ramires et al. (Ref 47) in their study evaluated the cell culture response of TiO_2/HA composite coatings (in different ratios) with primary rat osteoblasts cells and human osteoblast-like MG63 cell line. MTT tests revealed that TiO_2/HA coatings supported cell adhesion and proliferation on the both cell lines. There was no significant difference in cell proliferation behavior on the TiO_2/HA coatings after 7 days of incubation. In another study (Ref 48), Ca-P/TiO_2 hybrid coatings have been shown to exhibit increased proliferation of osteoblast-like cells compared to HA coatings or TiO_2 (rutile) surfaces. Earlier Liet al. (Ref 49) and Uchida et al. (Ref 50) reported that TiO_2 (anatase) had better ability to stimulate bone formation than TiO_2 (rutile).

In the present study, it has been observed that HA/TiO_2 bond coating with a higher roughness (R_a = 5.9±0.4 µm) had shown almost similar cell proliferation to HA-coated Ti-6Al-4V specimens having R_a value of 4.6 ± 0.2 µm, respectively. The un-coated Ti-6Al-4V (blasted) specimens having R_a value of 4.0 ± 0.4 µm showed a much lower cell proliferation than HA- and HA/TiO_2-coated specimens. It has been found that the cell proliferation behavior of the coated specimens is much better than the un-coated Ti-6Al-4V specimens after incubation in the culture media. There are also certain disagreements in literature data, about the effect of surface roughness on cell proliferation. It may be due to differences in the cell type used, culture conditions, serum concentration and surface fabrication methods (Ref 51). Lee et al. (Ref 52) in their study on plasma-sprayed HA coatings found that smooth surface (R_a = 0.67 µm) was more favorable to enhance the cell proliferation rate compared with the rough surface (R_a = 10.37µm).

Another study (Ref 53) shows that surface roughness of HA coatings significantly affects cell proliferation in comparison with the Ti coating on Ti-6Al-4V. Deligianni et al. (Ref 54) reported that cell adhesion, proliferation and detachment strength were surface roughness sensitive and increased as the roughness of HA increased. In the present study, better performances of the HA and HA/TiO_2 coatings may be due to their biological compatibility, bioactive characteristic and high crystallinity. Chou et al. (Ref 55) suggested that high crystalline HA coatings enhance cell proliferation while Ducheyne et al. (Ref 56) reported that

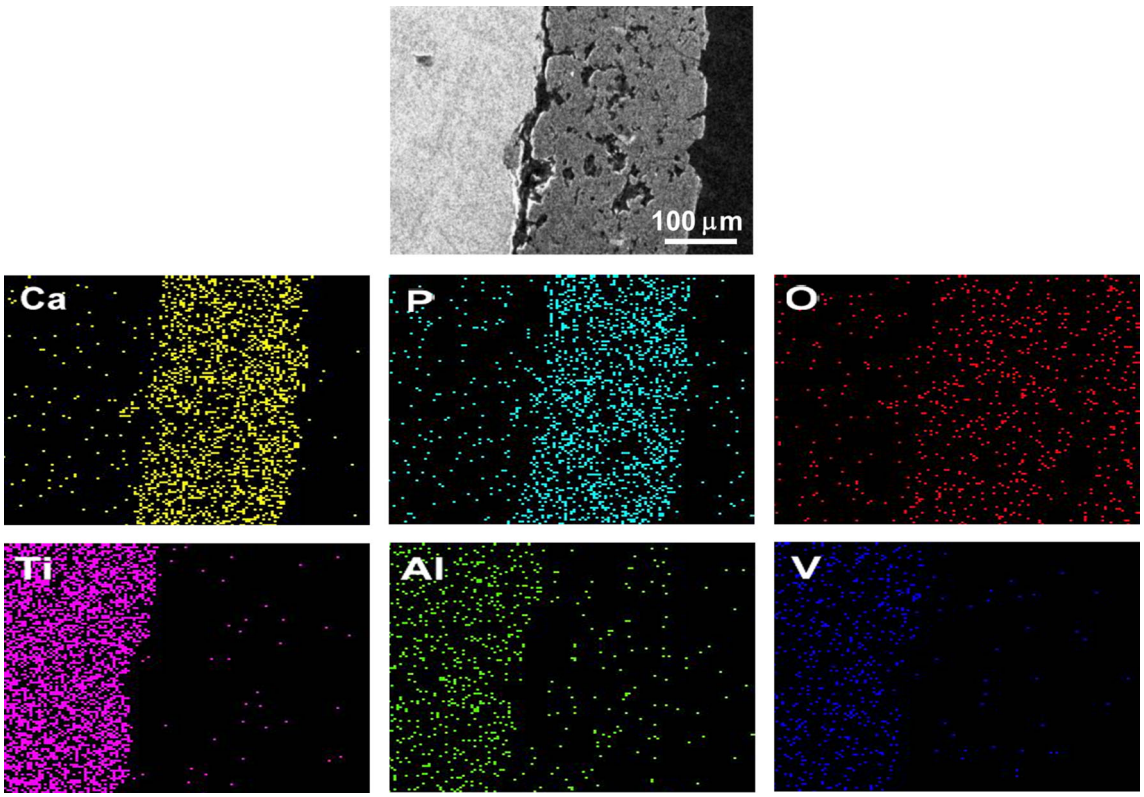

Fig. 11 Cross-sectional EDS elemental maps of flame-sprayed HA/TiO_2-coated Ti-6Al-4V alloy after immersion in Ringer's solution (scale bar = 100 µm)

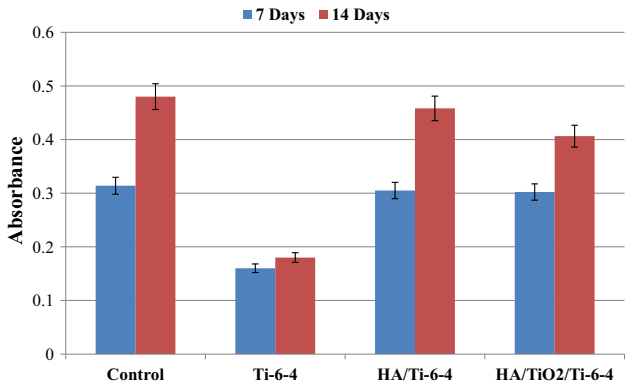

Fig. 12 MTT assay results of polystyrene culture plates (control), un-coated, flame-sprayed HA-coated (HA/Ti-6Al-4V), and HA/TiO_2-coated Ti-6Al-4V (HA/TiO_2/Ti-6Al-4V) specimens, after 7 and 14 days of incubation in culture medium. Each value and error bar represents the mean of triplicate samples and its standard deviation

highly crystalline HA coatings were beneficial for long-term survivability of different phases in bony tissues. Though HA and HA/TiO_2 coatings indicated a higher number of living cells in comparison with un-coated Ti-6Al-4V substrates, one important observation in this study is that surface roughness has not shown any significant effect on cell proliferation.

Conclusions

This study was conducted to analyze the biocompatibility and corrosion behavior of the Ti6Al4V alloy after the deposition of HA and HA/TiO_2 coatings. The following conclusions have been drawn from the study:

1. HA as well as HA/TiO_2 coatings were found to be useful to reduce the corrosion rates of the Ti-6Al-4V substrate materials in Ringer's solution at 37 ± 1 °C. XRD analysis of HA and HA/TiO_2 coatings before and after their immersion in Ringer's solution showed the presence of HA, with minor peaks for TTCP and β-TCP phases.
2. SEM/EDS analysis of HA- and HA/TiO_2-coated specimens before and after corrosion testing showed that the atomic percentage (%) of Ca and P got decreased, whereas that of O increased after their immersion in Ringer's solution. The coatings, in general, were intact and adherent to the base substrates even after exposure to Ringer's solution.
3. The HA/TiO_2 bond coatings were found to retain their identity even after corrosion testing. EDS point analysis confirmed that bond coat of TiO_2 was still covered with the HA top coat layers even after their exposure to Ringer's solution. Both investigated

coatings were found to retain their cross-sectional microstructure even after their exposure to the Ringer's solution.

4. In vitro cell culture studies showed that cells continued to proliferate favorably over a period of 14 days on both coatings. Surface roughness has not shown any significant effect on the cell proliferation. HA coating had shown a more favorable cellular response in terms of cell proliferation compared to un-coated and HA/TiO_2-bond-coated Ti-6Al-4V. Based on these observations, it was concluded that both HA as well as HA/TiO_2 bond coatings enhanced the biocompatibility and corrosion resistance of the Ti-6Al-4V implant material. HA coating showed better in vitro corrosion resistance and bioactivity compared to HA/TiO_2-coated and bare Ti-6Al-4V specimens.

References

1. K.K. Chew, S.H.S. Zein, and A.L. Ahmad, The Corrosion Scenario in Human Body: Stainless Steel 316L Orthopaedic Implants, *Nat. Sci.*, 2012, **4**(3), p 184-188
2. S.B. Goodman, Z. Yao, M. Keeney, and F. Yang, The Future of Biologic Coatings for Orthopaedic Implants, *Biomaterials*, 2013, **34**(13), p 3174-3183
3. G. Manivasagam, D. Dhinasekaran, and A. Rajamanickam, Biomedical Implants: Corrosion and its Prevention—A Review, *Recent Patents Corros. Sci.*, 2010, **2**, p 40-54
4. U.K. Mudali, T.M. Sridhar, and B. Raj, Corrosion of Bio Implants, *Sadhana*, 2003, **28**(3–4), p 601-637
5. I. Gurappa, Characterization of Different Materials for Corrosion Resistance under Simulated Body Fluid Conditions, *Mater. Charact.*, 2002, **49**(1), p 73-79
6. N. Hallab, K. Merritt, and J.J. Jacobs, Metal Sensitivity in Patients with Orthopaedic Implants, *J. Bone. Joint. Surg. Am.*, 2001, **83-A**(3), p 428-436
7. J.L. Gilbert, C.A. Buckley, and J.J. Jacobs, *In-Vivo* Corrosion of Modular Hip Prosthesis Components in Mixed and Similar Metal Combinations: The Effect of Crevice, Stress, Motion, and Alloy Coupling, *J. Biomed. Mater. Res.*, 1993, **27**(12), p 1533-1544
8. E.B. Mathiesen, J.U. Lindgren, G.G.A. Blomgren, and F.P. Reinholt, Corrosion of Modular Hip Prostheses, *J. Bone. Joint. Surg. Br.*, 1991, **73-B**(4), p 569-575
9. T.M. Grupp, T. Weik, W. Bloemer, and H.P. Knaebel, Modular Titanium Alloy Neck Adapter Failures in Hip Replacement-Failure Mode Analysis and Influence of Implant Material, *BMC Musculoskelet. Disord.*, 2010, **11**(3), p 1-12
10. J.R. Goldberg, J.L. Gilbert, J.J. Jacobs, T.W. Bauer, W. Paprosky, and S. Leurgans, A Multicenter Retrieval Study of the Taper Interfaces of Modular Hip Prostheses, *Clin. Orthop. Relat. Res.*, 2002, **401**, p 149-161
11. P.J. Hol, A. Molster, and N.R. Gjerdet, Should the Galvanic Combination of Titanium and Stainless Steel Surgical Implants be Avoided?, *Injury*, 2008, **39**(2), p 161-169
12. Q. Chen and G.A. Thouas, Metallic Implant Biomaterials, *Mater. Sci. Eng. R*, 2015, **87**, p 1-57
13. R.C. Rocha, A.G.S. Galdino, S.N. Silva, and M.L.P. Machado, Surface, Microstructural, and Adhesion Strength Investigations of a Bioactive Hydroxyapatite-Titanium Oxide Ceramic Coating Applied to Ti-6Al-4V Alloys by Plasma Thermal Spraying, *Mater. Res.*, 2018, **21**(4), p e20171144
14. R.B. Heimann, The Challenge and Promise of Low-Temperature Bioceramic Coatings: An Editorial, *Surf. Coat. Technol.*, 2016, **301**, p 1-5
15. J.L. Ong, M. Appleford, S. Oh, Y. Yang, W.H. Chen, J.D. Bumhardner, and W.O. Haggard, Characterization and Development of Bioactive Hydroxyapatite Coatings, *J. Miner. Met. Mater. Soc.*, 2006, **58**(7), p 67-69
16. S. Sobieszczyk, Surface Modifications of Ti and its Alloys, *Advanced Materials Science*, 2010, **10**(1), p 29-42
17. A. Killinger, P. Muller, and R. Gadow, What Do We Know, What are the Current Limitations of Suspension HVOF Spraying, *J. Therm. Spray Technol.*, 2015, **24**(7), p 1130-1142
18. P. Fauchais, M. Vardell, A. Vardelle, and S. Goutier, What Do We Know, What are the Current Limitations of Suspension Plasma Spraying?, *J. Therm. Spray Technol.*, 2015, **24**(7), p 1120-1129
19. T.P. Singh, H. Singh, and H. Singh, Characterization and In Vitro Investigations of Thermal Sprayed HA and HA/TiO_2 Coatings on 316L SS, *J. Thermal Spray Technol.*, 2012, **21**(5), p 917-927
20. X. Zhao, X. Liu, C. Ding, and P.K. Chu, In Vitro Bioactivity of Plasma-Sprayed TiO_2 Coating after Sodium Hydroxide Treatment, *Surf. Coat. Technol.*, 2006, **200**, p 5487-5492
21. T.P. Singh, H. Singh, and H. Singh, Characterization and In Vitro Corrosion Investigations of Thermal Sprayed Hydroxyapatite and Hydroxyapatite-Titania Coatings on Ti-Alloy, *Metall. Mater. Trans. A*, 2012, **43**(11), p 4365-4376
22. T.M. Sridhar, U.K. Mudali, and M. Subbaiyan, Sintering Atmosphere and Temperature Effects on Hydroxyapatite Coated Type 316L Stainless Steel, *Corros. Sci.*, 2003, **45**(10), p 2337-2359
23. Y. Yang, K. Kim, C.M. Agrawal, and J.L. Ong, Interaction of Hydroxyapatite-Titanium at Elevated Temperature in Vacuum Environment, *Biomaterials*, 2004, **25**(15), p 2927-2932
24. S. Lazic, S. Zec, N. Miljevic, and S. Milonjic, The Effect of Temperature on the Properties of Hydroxyapatite Precipitated from Calcium Hydroxide and Phosphoric Acid, *Thermochim. Acta*, 2001, **374**(1), p 13-22
25. P. Cheang and K.A. Khor, Addressing Processing Problems Associated with Plasma Spraying of Hydroxyapatite Coatings, *Biomaterials*, 1996, **17**(5), p 537-544
26. A.R. Boyd, B.J. Meenan, and N.S. Leyland, Surface Characterisation of the Evolving Nature of Radio Frequency (RF) Magnetron Sputter Deposited Calcium Phosphate Thin Films after Exposure to Physiological Solution, *Surf. Coat. Technol.*, 2006, **200**, p 6002-6013
27. T.F. Stoica, C. Morosanu, A. Slav, T. Stoica, P. Osiceanu, C. Anastasescu, M. Gartner, and M. Zaharescu, Hydroxyapatite Films Obtained by Sol-gel and Sputtering, *Thin Solid Films*, 2008, **516**, p 8112-8116
28. L.Q. Tri and D.H.C. Chua, An Investigation into the Effects of High Laser Fluence on Hydroxyapatite/Calcium Phosphate Films Deposited by Pulsed Laser Deposition, *Appl. Surf. Sci.*, 2009, **256**(1), p 76-80
29. R. d'Haese, L. Pawlowski, M. Bigan, R. Jaworski, and M. Martel, Phase Evolution of Hydroxapatite Coatings Suspension Plasma Sprayed Using Variable Parameters in Simulated Body Fluid, *Surf. Coat. Technol.*, 2010, **204**, p 1236-1246
30. R. Snyders, E. Bousser, D. Music, J. Jensen, S. Hocquet, and J.M. Schneider, Influence of the Chemical Composition on the Phase Constitution and the Elastic Properties of RF-Sputtered Hydroxyapatite Coatings, *Plasma Process. Polym.*, 2008, **5**(2), p 168-174
31. S. Kozerski, L. Pawlowski, R. Jaworski, F. Roudet, and F. Petit, Two Zones Microstructure of Suspension Plasma Sprayed

Hydroxyapatite Coatings Surf, *Coat. Technol.*, 2010, **204**, p 1380-1387
32. J. Legoux, F. Chellat, R. Lima, B. Marple, M. Bureau, H. Shen, and G. Candeliere, Development of Osteoblast Colonies on New Bioactive Coatings, *J. Thermal Spray Technol.*, 2006, **15**(4), p 628-633
33. K.A. Gross and D.M. Müller, Topography Control of Hydroxyapatite Coatings, *Key Eng. Mater.*, 2006, **309–311**, p 693-696
34. R.S. Lima, A. Kucuk, and C.C. Berndt, Evaluation of Microhardness and Elastic Modulus of Thermally Sprayed Nanostructured Zirconia Coatings, *Surf. Coat. Technol.*, 2001, **135**(2–3), p 166-172
35. T.P. Singh, H. Singh, and H. Singh, Characterization of Thermal Sprayed Hydroxyapatite Coatings on Some Biomedical Implant Materials, *J. Appl. Biomater. Funct. Mater.*, 2014, **12**(1), p 48-56
36. S.K. Yen, S.H. Chiou, S.J. Wu, C.C. Chang, S.P. Lin, and C.M. Lin, Characterization of Electrolytic HA/ZrO_2 Double Layers Coatings on Ti-6Al-4V Implant Alloy, *Mater. Sci. Eng.*, 2006, **26**(1), p 65-77
37. M.H. Fathi, M. Salehi, A. Saatchi, V. Mortazavi, and S.B. Moosavi, In Vitro Corrosion Behavior of Bioceramic, Metallic and Bioceramic-Metallic, Coated Stainless Steel Dental Implants, *Dent. Mater.*, 2003, **19**(3), p 188-198
38. S.C.P. Cachinho and R.N. Correia, Titanium Scaffolds for Osteointegration: Mechanical, In Vitro and Corrosion Behavior, *J. Mater. Sci. Mater. Med.*, 2008, **19**(1), p 451-457
39. R. Kumari and J.D. Majumdar, Studies on Corrosion Resistance and Bio-Activity of Plasma Spray Deposited Hydroxylapatite (HA) based TiO_2 and ZrO_2 Dispersed Composite Coatings on Titanium Alloy (Ti-6Al-4V) and the Same after Post Spray Heat Treatment, *Appl. Surf. Sci.*, 2017, **420**, p 935-943
40. C.T. Kwok, P.K. Wong, F.T. Cheng, and H.C. Man, Characterization and Corrosion behavior of Hydroxyapatite Coatings on Ti6Al4V Fabricated by Electrophoretic Deposition, *Appl. Surf. Sci.*, 2009, **255**(13–14), p 6736-6744
41. M.H. Fathi and F. Azam, Novel Hydroxyapatite/Tantalum Surface Coating for Metallic Dental Implant, *Mater. Lett.*, 2007, **61**(4–5), p 1238-1241
42. I.C. Lavos-Valereto, I. Costa, and S. Wolynec, The Electrochemical Behavior of Ti-6Al-7Nb Alloy with and without Plasma-Sprayed Hydroxyapatite Coating in Hank's Solution, *J. Biomed. Mater. Res.*, 2002, **63**(5), p 664-670
43. H. Kim, R.P. Camata, Y.K. Vohra, and W.R. Lacefield, Control of Phase Composition in Hydroxyapatite/Tetracalcium Phosphate Biphasic Thin Coatings for Biomedical Applications, *J. Mater. Sci. Mater. Med.*, 2005, **16**(10), p 961-966
44. Y.P. Lu, Y.Z. Song, R.F. Zhu, M.S. Li, and T.Q. Lei, Factors Influencing Phase Compositions and Structure of Plasma Sprayed Hydroxyapatite Coatings During Heat Treatment, *Appl. Surf. Sci.*, 2003, **206**(1), p 345-354
45. S. Mohanty, Y.K. Inchara, J.A. Crasta, and A. Ananthamurthy, An Unusual Case of Primary Osteosarcoma of the Rib in an Adult, *Indian J. Med. Paediatr. Oncol.*, 2010, **31**(1), p 18-20
46. A.T. Rad, M. Solati-Hashjin, N.A.A. Osman, and S. Faghihi, Improved Bio-Physical Performance of Hydroxyapatite Coatings obtained by Electrophoretic Deposition at Dynamic Voltage, *Ceram. Int.*, 2014, **40**(8), p 12681-12691
47. P.A. Ramires, F. Cosentino, E. Milella, P. Torricelli, G. Giavaresi, and R. Giardino, In Vitro Response of Primary Rat Osteoblasts to Titania/Hydroxyapatite Coatings Compared with Transformed Human Osteoblast-Like Cells, *J. Mater. Sci. Mater. Med.*, 2002, **13**(8), p 797-801
48. A.R. Boyd, G.A. Burke, H. Duffy, M.L. Cairns, P. O'Hare, and B.J. Meenan, Characterization of Calcium Phosphate/Titanium Dioxide Hybrid Coatings, *J. Mater. Sci. Mater. Med.*, 2008, **19**(2), p 485-498
49. P. Li, I. Kangasniemi, K. De Groot, and T. Kokubo, Bonelike Hydroxyapatite Induction by a Gel Derived Titania on a Titanium Substrate, *J. Am. Ceram. Soc.*, 1994, **77**(5), p 1307-1312
50. M. Uchida, H.M. Kim, T. Kokubo, S. Fujibasyashi, and T. Nakamura, Structural Dependence of Apatite Formation on Titania Gels in a Simulated Body Fluid, *J. Biomed. Mater. Res. A*, 2003, **64**(1), p 164-170
51. T. Osathanon, K. Bespinyowong, M. Arksornnukit, H. Takahashi, and P. Pavasant, Human Osteoblast-Like Cell Spreading and Proliferation on Ti-6Al-7Nb Surfaces of Varying Roughness, *J. Oral Sci.*, 2011, **53**(1), p 23-30
52. T.M. Lee, R.S. Tsai, E. Chang, C.Y. Yang, and M.R. Yang, The Cell Attachment and Morphology of Neonatal Rat Calvarial Osteoblasts on the Surface of Ti6Al4V and Plasma Sprayed HA Coating: Effect of Surface Roughness and Serum Contents, *J. Mater. Sci. Mater. Med.*, 2002, **13**(4), p 341-350
53. V. Borsari, G. Giavaresi, M. Fini, P. Torricelli, A. Salito, R. Chiesa, L. Chiusoli, A. Volpert, L. Rimondini, and R. Giardino, Physical Characterization of Different-Roughness Titanium Surfaces, with and without Hydroxyapatite Coating, and their Effect on Human Osteoblast-like Cells, *J. Biomed. Mater. Res. B Appl. Biomater.*, 2005, **75**(2), p 359-368
54. D.D. Deligianni, N.D. Katsala, P.G. Koutsoukos, and Y.F. Missirlis, Effect of Surface Roughness of Hydroxyapatite on Human Bone Marrow Cell Adhesion, Proliferation, Differentiation and Detachment Strength, *Biomaterials*, 2001, **22**(1), p 87-96
55. L. Chou, B. Marek, and W.R. Wagner, Effects of Hydroxylapatite Coating Crystallinity on Biosolubility, Cell Attachment Efficiency and Proliferation In Vitro, *Biomaterials*, 1999, **20**(10), p 977-985
56. P. Ducheyne, S. Radin, and L. King, The Effect of Calcium Phosphate Ceramic Composition and Structure on In Vitro Behavior. I. Dissolution, *J. Biomed. Mater. Res.*, 1993, **17**, p 25-34